Abrasive waterjet machining of three-dimensional structures from bulk metallic glasses and comparison with other techniques

Victor Wessels
Laboratory of Metal Physics and Technology, Department of Materials, ETH Zurich, 8093 Zurich, Switzerland

Anton Grigoryev
INSPIRE AG, 8092 Zurich, Switzerland; and Institute of Machine Tools and Manufacturing (IWF), ETH Zurich, 8092 Zurich, Switzerland

Claus Dold, Carl-Frederik Wyen, and Raoul Roth
INSPIRE AG, 8092 Zurich, Switzerland

Eduardo Weingärtner
Institute of Machine Tools and Manufacturing (IWF), ETH Zurich, 8092 Zurich, Switzerland

Frank Pude
INSPIRE AG, 8092 Zurich, Switzerland

Konrad Wegener
INSPIRE AG, 8092 Zurich, Switzerland; and Institute of Machine Tools and Manufacturing (IWF), ETH Zurich, 8092 Zurich, Switzerland

Jörg F. Löffler[a)]
Laboratory of Metal Physics and Technology, Department of Materials, ETH Zurich, 8093 Zurich, Switzerland

(Received 25 October 2011; accepted 23 January 2012)

Bulk metallic glasses (BMGs) are a promising class of engineering materials, but they can be difficult to machine due to high hardness and a metastable structure. Crystallization due to machining can have negative effects, such as a decreased load-bearing capacity of fabricated parts, and thus should be avoided. Here, a Zr-based BMG was machined using abrasive waterjet (AWJ), electrical discharge, ns-pulsed laser engraving, and conventional dry-milling techniques. Characterization of the processed material indicated that AWJ preserves the amorphous phase and provides the combination of speed and flexibility required to rapidly fabricate small three-dimensional parts, while the other techniques did not achieve these goals. As proof-of-principle, a screw, similar to an orthopedic implant, was rapidly machined from the BMG using AWJ.

I. INTRODUCTION

Certain alloy melts can be solidified without crystallization, producing an amorphous alloy or metallic glass. In the case of small critical cooling rates (1–100 K/s), amorphous specimens with a critical dimension ranging from 1 mm to a few centimeters can be produced by conventional die-casting.[1] Bulk metallic glasses (BMGs) possess desirable mechanical, magnetic, thermophysical, and corrosion properties[2,3] that make them attractive for a variety of applications including biomedical implants.[4,5] The amorphous state is metastable, which limits the amount of heat and/or strain that can be applied during a process such as machining. Crystallization or structural relaxation of the glass may negatively affect the properties of a machined part by, e.g., reducing the load-bearing capacity. Alternatives to machining, such as net-shape casting,[6] thermoplastic forming,[7] and blow molding[8] have been used to produce complex parts from BMGs. These methods, however, also have drawbacks: net-shape casting of complex parts generates high shear stresses in the melt, which can induce crystallization or create flow defects in the part; thermoplastic forming and blow molding can be performed on limited timescales only and may be applied only to BMGs with high thermal stability. Thus, machining methods that are "nondestructive" with respect to the amorphous phase and that offer many degrees of freedom are needed to extend the application of BMGs.

Machining of Zr-based BMGs by milling,[9] turning,[10,11] or drilling[12] has been studied. The respective studies report that temperatures up to 2700 K may arise and that damage to cutting tools, due to the high hardness of the BMG, can occur. The effects of laser micromachining of a Zr–Cu–Al BMG with a CO_2 laser have been examined,[13] showing formation of crystalline grains in the heat-affected zone and contraction due to recrystallization in the melted zone. Noncontact micro-electrical discharge

[a)]Address all correspondence to this author.
e-mail: joerg.loeffler@mat.ethz.ch
DOI: 10.1557/jmr.2012.36

machining (EDM) of the surface of a BMG has also been explored[14,15] and was found to be nondestructive.

Abrasive waterjet (AWJ) machining[16] is an attractive alternative to the above methods. In AWJ, a mixture of water and abrasive material (usually garnet granules of around 1–2 μm diameter with variable concentration in the mixture) is ejected at high pressure (typically between 1 and 10 kbar) through a focusing nozzle, producing a cutting jet that can be used to machine a wide variety of materials including ceramics, metals, wood, and plastic. Local heating is minimal with this method, making it attractive for machining heat-sensitive materials. In a five-axis configuration with computer numerical control (CNC), it can be used to machine complex three-dimensional (3D) shapes. To our knowledge, a detailed study of AWJ on BMGs has not yet been reported.

In the present study, four methods—milling, ns-pulsed laser cutting, wire-EDM, and AWJ—were used to machine a Zr-based BMG. The processed specimens were analyzed by scanning electron microscopy (SEM), x-ray diffraction (XRD), and differential scanning calorimetry (DSC). From these results, and from comparison to previous reports, AWJ was determined to be the optimal method of nondestructive machining of BMGs to produce complex parts. As proof-of-principle, a prototypical screw was machined from the BMG using AWJ.

II. EXPERIMENTAL METHODS

Amorphous samples of $Zr_{52.5}Cu_{17.9}Ni_{14.6}Al_{10}Ti_5$ (Vitreloy 105[17]; all values in at. %) were prepared in various geometries by two methods: radio-frequency induction melting and gravity casting into a Cu mold, or suction casting during electrical arc melting on a water-cooled Cu hearth. The gravity casting method produced plates with nominal dimensions of 65 × 43 × 3 mm^3; suction casting with various molds produced cylinders of either 2 or 4 mm diameter and 30 mm length. The plates were machined by four methods: conventional dry milling on a Mikron VC 1000 (The Mikron Group, Agno, Switzerland) machining center at cutting speeds of 20 and 200 m/min using a straight cemented carbide tool (ISO K10); wire-EDM in a deionized water dielectric with values of peak current varied from 100 to 380 A, pulling force of 13 N, impulse times ranging from 1 to 2.5 μs, frequency of 10 kHz, and open voltage of 85 V; AWJ with a garnet abrasive mixture at a constant flow rate of 170 g/min, pressure of 2400 bar, a nozzle of 0.5 mm diameter at its exit, and feed rates varying from 300 to 1000 mm/min (see also Fig. 1); ns-pulsed laser structuring (average maximum output power 18 W) performed at various combinations of feed rate varied from 100 to 1900 mm/s and output power varied from 10 to 100%, with pulse frequencies of 30, 65, and 100 kHz. During AWJ, thermal radiation images were captured using an infrared camera.

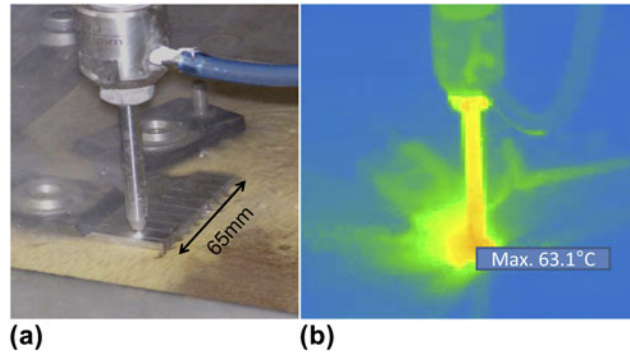

FIG. 1. (a) A photograph of the setup used for cutting the Zr-based bulk metallic glasses (BMG) plates by abrasive waterjet (AWJ) machining and (b) thermal image taken during cutting of a BMG plate, with a maximum temperature of 63.1 °C.

The as-cast and machined samples were examined by XRD, using Cu Kα (λ = 0.15406 nm) radiation in a Bragg–Brentano geometry, and SEM using a Hitachi SU-70 (Hitachi High Technologies America, Inc., Pleasanton, CA) operated at 20 kV. Sections of 5 mm length were cut from the 2 mm diameter rods by AWJ at speeds of 400, 500, and 1000 mm/min, and analyzed by DSC during linear heating at a rate of 5 K/min using a Netzsch model 404 DSC (Netzsch GmbH, Selb, Germany). Chips produced by milling were analyzed in a Seiko Instruments 220CU DSC (Seiko Instruments, Chiba, Japan). The screw prototypes were machined from the 4-mm BMG rods by AWJ with a 0.6-mm focusing nozzle while fixed in a rotating chuck (see also Fig. 5 and related discussion).

III. RESULTS AND DISCUSSION

Figure 1(a) shows the setup used for AWJ of the BMG plates, and Fig. 1(b) shows a thermal image obtained during cutting of the plates. From an analysis of the thermal images, the maximum temperature was 63.1 °C, indicating that this process could be used to machine most BMGs without thermal damage.

Figure 2 shows SEM images of the surfaces resulting from AWJ and wire-EDM. Figure 2(a) shows the surface after machining by waterjet cutting at a feed rate of 1000 mm/min. The effects of broadening of the jet are evident from a slight change in roughness along the cutting direction (indicated by the black arrow); this effect was observed for all speeds. Figure 2(c) shows a magnification of the lower portion of the cut zone in (a), where grooves 1–2 μm wide produced by the abrasive can be seen. Similar images for wire-EDM cutting are provided in Fig. 2(b) and its inset (although no directional effects are present for EDM). From Fig. 2(b), it is evident that EDM produced a surface composed of agglomerations of micrometer sized, approximately spherical particles. The formation and structure of the surface produced by EDM is discussed in more detail below. The surface morphologies resulting from both methods depicted in Figs. 2(a) and 2(b)

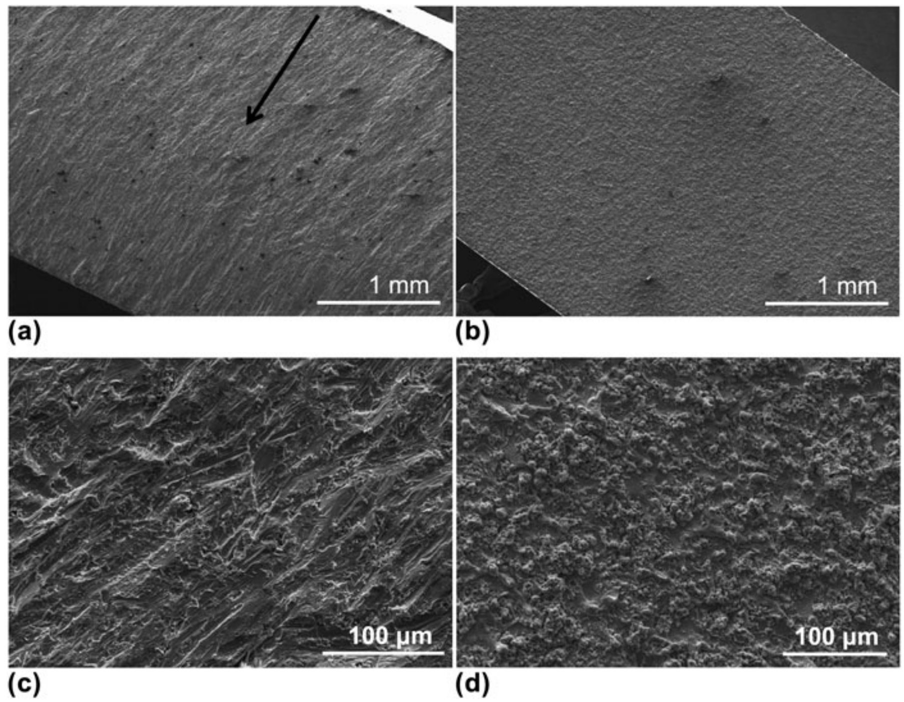

FIG. 2. Representative scanning electron microscopy images of machined BMG surfaces using (a) AWJ (1000 mm/min feed rate) and (b) electrical discharge machining (EDM) at 380 A; (c) and (d) are higher magnification images of the surfaces from (a) and (b), respectively; the surface in (b, d) appears to be partially crystallized (see Fig. 4 and discussion in the text). The arrow in (a) indicates the direction of the jet; effects of jet-broadening can be seen by a slight change in surface finish along the direction of the jet.

were representative of all parameter sets studied for those techniques; slight changes in roughness could be seen, but they did not depend systematically on machine parameters.

Figure 3 shows grooves engraved by ns-pulsed laser micromachining with different combinations of output power and feed rate, at a fixed pulse frequency of 30 kHz. Figures 3(a) and 3(b) show engravings made with 100 and 1000 mm/s feed rate, respectively, with power fixed at 10%; Figs. 3(c) and 3(d) are for the same speeds, with the power increased to 70%. Dramatic differences in the morphology of the cut surfaces can be seen for the different conditions. At lower power, increasing the feed rate resulted in overlapped individual melted spots of around 40 μm diameter [Fig. 3(b)]. The ripple patterns indicate contraction of the material upon solidification of the melted zone, owing to crystallization. Since the density of the amorphous phase is similar to that of the liquid, such contraction would not occur if the recast zone were amorphous. Increasing output power to 70% resulted in prominent damage from recasting and deposition of melted material [Figs. 3(c) and 3(d)]. From these results, we conclude that the particular method of laser machining studied here is not suitable for structuring of these BMGs without thermal damage. Implementation of more sophisticated methods using ultrashort laser pulses may still be useful for structuring BMGs; additional work on this topic is proceeding.

Figure 4(a) shows representative XRD spectra for the BMG in the as-cast state and after cutting by AWJ, EDM, and milling (AWJ at 1000 mm/min and EDM using 380 A are shown, and are representative of all AWJ and EDM conditions). The absence of Bragg peaks suggests that AWJ did not induce crystallization, while the spectrum after cutting by wire-EDM shows numerous such reflections along with an amorphous background, indicating partial crystallization. That figure also shows the XRD spectra of chips from dry milling at cutting speeds of 20 and 200 m/min. The former condition shows no Bragg peaks, while the latter shows many, which indicates total crystallization. When milling at a cutting speed of 200 m/min, flashes of burning chips were often observed, suggesting that temperatures above 2400 K occurred at the interface.[11] These results suggest that this BMG can be reliably machined by dry milling only if low cutting speeds (around 20 m/min) are used, which is consistent with previous reports.[10] Figure 4(b) shows DSC traces of the BMG as-cast and after machining by AWJ, at various feed rates, and EDM at 380 A (representative of DSC for all EDM conditions). The as-cast BMG shows similar results to those reported elsewhere for the same composition (including the dual overlapping peaks during primary crystallization, which are due to nanometer scale heterogeneities[18]). No changes outside of experimental uncertainty can be seen for the machined samples, further supporting the claim that AWJ is nondestructive. This also suggests that the crystallization observed by XRD for the EDM cuts is predominantly on the surface.

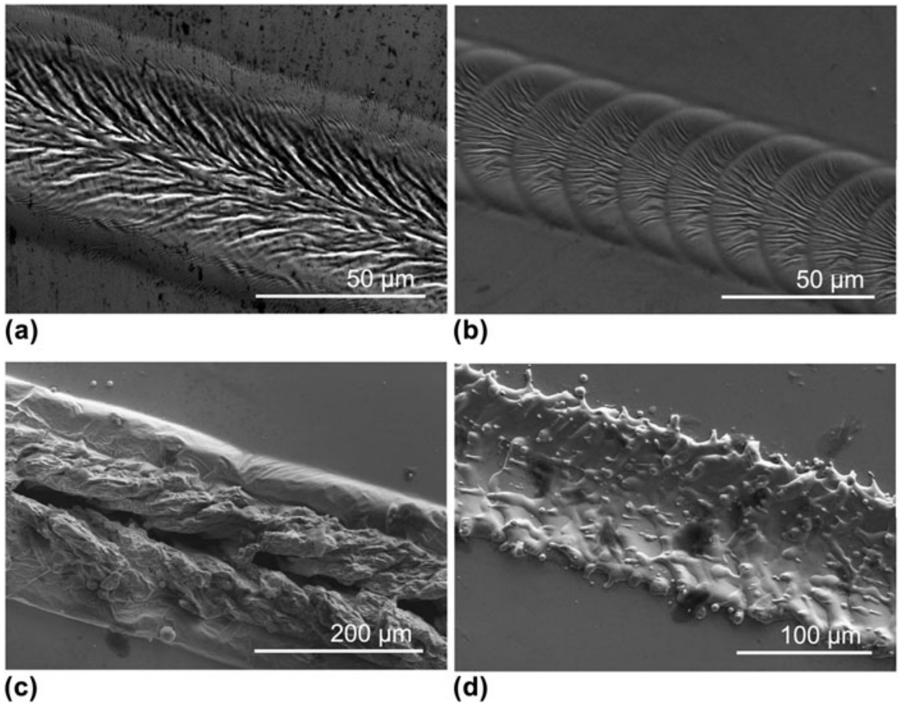

FIG. 3. Grooves engraved into the surface of the BMG by a ns-pulsed laser at (a, b) 100 and 1000 mm/s feed rates, respectively, and 10% power; (c, d) 100 and 1000 mm/s, respectively, and 70% power. In (a, b), contraction due to crystallization is indicated by the rippled morphology; in (c, d), extreme surface damage and redeposition of melted material are seen.

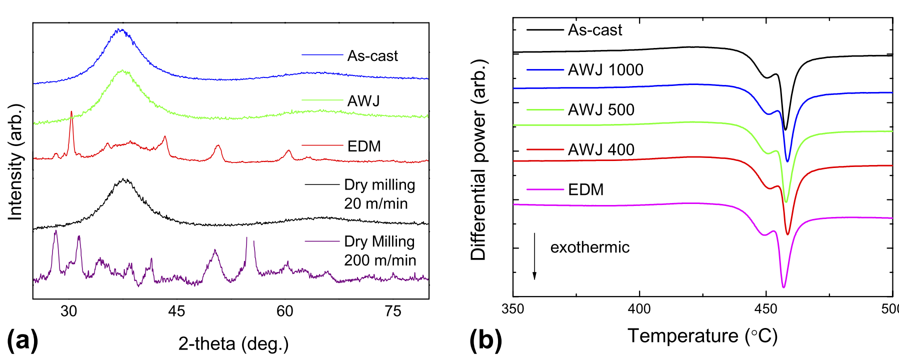

FIG. 4. (a) Representative x-ray diffraction (XRD) traces of the BMG as-cast, after machining by AWJ (1000 mm/min feed rate), EDM (380 A), and dry milling at cutting speeds of 20 and 200 m/min (XRD traces from chips). Surface crystallization from EDM can be seen although none is observed from AWJ; the chips from milling with 200 m/min cutting speed show complete crystallization (an intense peak at $2\theta = 55°$ was truncated to preserve the scale) while with 20 m/min they do not; (b) differential scanning calorimetry (DSC) traces for the BMG as-cast and after machining, by AWJ at various speeds and EDM at 380 A, showing no changes outside normal variance. DSC traces for the milled chips (not shown) confirm the XRD results from (a) for those samples.

The agglomerated particles observed from SEM (Fig. 2) may arise from local melting and recrystallization and may thus be the source of the Bragg reflections. DSC performed on the chips from milling at 20 and 200 m/min was consistent with the XRD traces of Fig. 4(a): the chips produced by the higher cutting speed show no glass transition and no distinct crystallization event, indicating that they have been fully crystallized.

Figure 5 shows the setup used to machine the prototype screw from the rod-shaped BMG using AWJ; the insets to Fig. 5 show a detail of the screw threads and the XRD spectrum of the finished part. The flash of light seen near the jet was due to a chemical reaction of Ti with air. This is observed when machining alloys containing Ti with a waterjet. This effect should not be confused with the flash generated during, e.g., milling, which is associated with extremely high temperatures. From the photograph of the screw, it can be seen that the threads are uniform and smooth. From the XRD trace, no Bragg reflections are present, suggesting that crystallization did not occur. DSC scans were also performed on sections of the screw (not shown) and showed no change compared to the as-cast

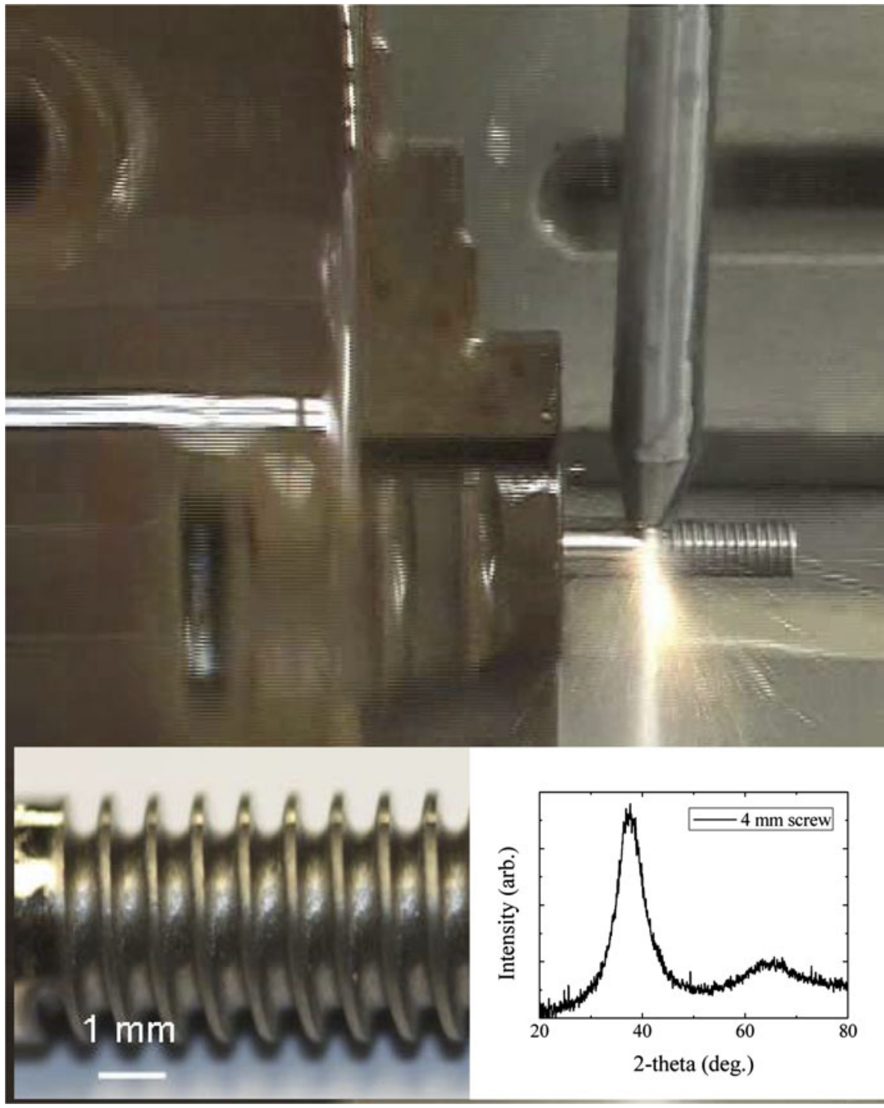

FIG. 5. An image captured from video of the setup for fabricating a prototype screw from the 4-mm BMG pin using AWJ. The insets show a higher magnification photograph of the finished part and the XRD spectrum of the screw, which exhibits no Bragg peaks, indicating that crystallization did not occur. The video of the machining process can be found in the supplementary material accompanying the online version of the article.

BMG. (A video of the machining process is available as supplementary material attached to the online version of this article.) Corrosion caused by the waterjet was not investigated in this study. The results of DSC and XRD measurements, however, suggest that this was not a concern for this BMG. For other BMGs that are highly susceptible to corrosion in aqueous solutions, or for parts needed in corrosive environments, further investigation of corrosion may be required.

IV. CONCLUSIONS

Conventional dry milling, wire-EDM, ns-pulsed laser micromachining, and AWJ machining were evaluated as methods for machining a Zr-based BMG, with the aim of producing complex 3D devices such as orthopedic screws or other load-bearing implants. AWJ machining showed the best combination of low process temperatures, high feed rates, and degrees of freedom needed to fabricate 3D parts. The other techniques have various limitations, such as lower potential feed rates, tool damage, fewer degrees of freedom, or crystallization induced at the surface. As proof-of-principle, AWJ was used to fabricate a prototypical screw from a 4-mm-diameter BMG rod. The machining setup (Fig. 5) could be modified and CNC incorporated to fabricate a true orthopedic implant.

It should be noted that the Zr-based BMG used here has high glass-forming ability (GFA) and thermal stability, which make it suitable for plastic-forming and net shape-casting operations. Based on its high GFA, this

BMG was chosen for evaluating new machining techniques, which was the goal of this study. The results presented here indicate that AWJ is a very promising method for machining BMGs. It enables rapid fabrication of 3D parts from BMGs that are typically difficult to machine or form, such as those with lower thermal stability.

ACKNOWLEDGMENTS

V. Wessels and J.F. Löffler thank Erwin Fischer and Beatrice Wegmann for help with preparation of the amorphous samples.

REFERENCES

1. A. Inoue: Stabilization of metallic supercooled liquid and bulk amorphous alloys. *Acta Mater.* **48**(1), 279 (2000).
2. J.F. Löffler: Bulk metallic glasses. *Intermetallics* **11**(6), 529 (2003).
3. W.H. Wang, C. Dong, and C.H. Shek: Bulk metallic glasses. *Mater. Sci. Eng., R* **44**(2–3), 45 (2004).
4. B. Zberg, P.J. Uggowitzer, and J.F. Löffler: MgZnCa glasses without clinically observable hydrogen evolution for biodegradable implants. *Nat. Mater.* **8**(11), 887 (2009).
5. J. Schroers, G. Kumar, T.M. Hodges, S. Chan, and T.R. Kyriakides: Bulk metallic glasses for biomedical applications. *JOM* **61**(9), 21 (2009).
6. W.L. Johnson: Bulk amorphous metal—An emerging engineering material. *JOM* **54**(3), 40 (2002).
7. J. Schroers: On the formability of bulk metallic glass in its supercooled liquid state. *Acta Mater.* **56**(3), 471 (2008).
8. J. Schroers, Q. Pham, A. Peker, N. Paton, and R.V. Curtis: Blow molding of bulk metallic glass. *Scr. Mater.* **57**(4), 341 (2007).
9. M. Bakkal and V. Naksiler: Cutting mechanics of bulk metallic glass materials on meso-end milling. *Mater. Manuf. Processes* **24**(12), 1249 (2009).
10. M. Bakkal, A.J. Shih, R.O. Scattergood, and C.T. Liu: Machining of a Zr–Ti–Al–Cu–Ni metallic glass. *Scr. Mater.* **50**(5), 583 (2004).
11. M. Bakkal, C.T. Liu, T.R. Watkins, R.O. Scattergood, and A.J. Shih: Oxidation and crystallization of Zr-based bulk metallic glass due to machining. *Intermetallics* **12**(2), 195 (2004).
12. M. Bakkal, A.J. Shih, S.B. McSpadden, and R.O. Scattergood: Thrust force, torque, and tool wear in drilling the bulk metallic glass. *Int. J. Mach. Tools Manuf.* **45**(7–8), 863 (2005).
13. S.N. Aqida, D. Brabazon, S. Naher, Z. Kovacs, and D.J. Browne: Laser micro-processing of amorphous and partially crystalline Cu45Zr48Al7 alloy. *Appl. Phys. A Mater.* **101**(2), 357 (2010).
14. S.H. Yeo, P.C. Tan, A. Erwin, S.B. Tor, and N.H. Loh: Processing of zirconium-based bulk metallic glass (BMG) using micro electrical discharge machining (Micro-EDM). *Mater. Manuf. Processes* **24**(12), 1242 (2009).
15. X.H. Chen, X.C. Zhang, Y. Zhang, and G.L. Chen: Fabrication and characterization of metallic glasses with a specific microstructure for micro-electro-mechanical system applications. *J. Non-Cryst. Solids* **354**(28), 3308 (2008).
16. A.W. Momber and R. Kovacevic: *Principles of Abrasive Water Jet Machining* (Springer, Berlin, 1998).
17. X.H. Lin, W.L. Johnson, and W.K. Rhim: Effect of oxygen impurity on crystallization of an undercooled bulk glass forming Zr-Ti-Cu-Ni-Al alloy. *Mater. Trans. JIM* **38**(5), 473 (1997).
18. E. Pekarskaya, J.F. Löffler, and W.L. Johnson: Microstructural studies of crystallization of a Zr-based bulk metallic glass. *Acta Mater.* **51**(14), 4045 (2003).

Supplementary Material

Supplementary material can be viewed in this issue of the *Journal of Materials Research* by visiting http://journals.cambridge.org/jmr.